EUKARYOTIC CELL, Apr. 2005, p. 765–774 Vol. 4, No. 4
1535-9778/05/$08.00+0 doi:10.1128/EC.4.4.765–774.2005

Mitochondrial DNA Ligases of *Trypanosoma brucei*

Nick Downey,† Jane C. Hines, Krishna M. Sinha, and Dan S. Ray*

Molecular Biology Institute and Department of Microbiology, Immunology, and Molecular Genetics, University of California, Los Angeles, California

Received 23 December 2004/Accepted 26 January 2005

The mitochondrial DNA of *Trypanosoma brucei*, termed kinetoplast DNA or kDNA, consists of thousands of minicircles and a small number of maxicircles catenated into a single network organized as a nucleoprotein disk at the base of the flagellum. Minicircles are replicated free of the network but still contain nicks and gaps after rejoining to the network. Covalent closure of remaining discontinuities in newly replicated minicircles after their rejoining to the network is delayed until all minicircles have been replicated. The DNA ligase involved in this terminal step in minicircle replication has not been identified. A search of kinetoplastid genome databases has identified two putative DNA ligase genes in tandem. These genes (*LIG kα* and *LIG kβ*) are highly diverged from mitochondrial and nuclear DNA ligase genes of higher eukaryotes. Expression of epitope-tagged versions of these genes shows that both LIG kα and LIG kβ are mitochondrial DNA ligases. Epitope-tagged LIG kα localizes throughout the kDNA, whereas LIG kβ shows an antipodal localization close to, but not overlapping, that of topoisomerase II, suggesting that these proteins may be contained in distinct structures or protein complexes. Knockdown of the *LIG kα* mRNA by RNA interference led to a cessation of the release of minicircles from the network and resulted in a reduction in size of the kDNA networks and rapid loss of the kDNA from the cell. Closely related pairs of mitochondrial DNA ligase genes were also identified in *Leishmania major* and *Crithidia fasciculata*.

Trypanosoma brucei is a parasitic protozoan and the etiologic agent of severe diseases of humans and livestock in sub-Saharan Africa (2). Understanding the fundamental biology of these early diverging eukaryotes is important for both public health and economic growth in these areas. *T. brucei* has also proved to be a valuable model system for understanding basic eukaryotic cell biology (11). Several important cellular processes described first for *T. brucei* either have been found in other eukaryotes, e.g., glucosyl phosphatidylinositol anchoring of proteins (15) and RNA editing (28), or are still apparently unique to kinetoplastids and give an indication of evolutionary divergence, e.g., their unique form of mitochondrial DNA (19).

The mitochondrial genome of these parasites is highly unusual. It is termed the kinetoplast DNA (kDNA) and consists of 25 to 35 circular DNA molecules (maxicircles) and, in addition, several thousand smaller circular molecules (minicircles). The minicircles encode guide RNAs utilized in editing of maxicircle transcripts by a mechanism involving the insertion and/or deletion of U residues (20, 29). Minicircles are catenated into a large network through which the maxicircles are interwoven (19). The complex of interwoven circles of DNA are compacted together to form a disk shape, the thickness of which is roughly equivalent to the length of a minicircle stretched taut (16).

Current understanding of the process of kDNA replication has come from studies carried out largely with *Crithidia fasciculata* and *T. brucei*. Minicircles are released from the network in a vectoral manner prior to replication (6), and free minicircles are detected on the flagellar side of the kDNA disk. Molecular analysis of replication intermediates indicates that minicircle replication occurs in a unidirectional manner from a single origin of replication (although in *C. fasciculata* there are two origin sites per minicircle) (4). Several DNA polymerases have been localized to the mitochondrion recently, and one or more of these are likely to be involved in the replication of the kDNA minicircles (17). Rejoining of nascent minicircles to the kDNA network occurs at antipodal sites flanking the kDNA disk (9, 25) and involves a kinetoplast-specific DNA topoisomerase (21). An RNase HI-like enzyme structure-specific endonuclease I localizes to antipodal sites (7) and has been implicated in RNA primer removal (14). DNA polymerase β is also found at the antipodal sites and is implicated in filling the gaps left after primer removal (14). These nicked and gapped minicircles are reattached to the network by the topoisomerase II. However, a single nick or gap remains at the minicircle origin until all the minicircles have been duplicated (23, 24). Minicircles are removed from the interior of the disk and replicated free of the network (8). Thus, as replication of the disk continues, the newly replicated minicircles accumulate at the antipodal sites of reattachment, but in *T. brucei*, the nascent minicircles do not distribute around the perimeter of the network as in the case of *C. fasciculata* (10, 25, 26). When all of the minicircles have been replicated, all of the nicks in the minicircles are covalently closed and the disk is then segregated into two daughter networks by unknown mechanisms (24).

One enzyme activity that is essential for the completion of DNA replication and is missing from this description is DNA ligase. There are two stages in the minicircle replication process at which DNA ligase is required. The first is in sealing Okazaki fragments in the discontinuously synthesized DNA strand. The second is in the final sealing of minicircles that

* Corresponding author. Mailing address: Paul D. Boyer Hall, 611 Charles Young Dr., University of California, Los Angeles, CA 90095-1570. Phone: (310) 825-4178. Fax: (310) 206-7286. E-mail: danray@ucla.edu.

† Present address: Department of Biology, Luther College, Decorah, Iowa.

marks the end of kDNA replication and immediately precedes segregation of the daughter kDNA disks. We have recently described a novel DNA ligase (which we now call LIG kβ) from *C. fasciculata* that localizes to the antipodal sites of the kDNA (30). This protein coimmunoprecipitates with DNA polymerase β, suggesting that it is involved in the repair of Okazaki fragments in nascent minicircles at the antipodal sites. In this report, we describe the *T. brucei* homologue of LIG kβ and a second *T. brucei* DNA ligase (LIG kα) that localizes throughout the kDNA. Upon RNA interference (RNAi) knockdown of *LIG kα*, there is a rapid cessation of cell division, a depletion of the pool of free covalently closed minicircles, and an accumulation of nicked or gapped minicircles within the networks. The inhibition of ligation of discontinuities in the minicircles is followed by loss of the kDNA. We suggest that LIG kα may be responsible for the final sealing of minicircles before segregation of the replicated DNA.

MATERIALS AND METHODS

Gene discovery and cloning. An open reading frame (ORF) identified as a DNA ligase (*LIG kα* gene) was discovered in a GeneDB contig (Tb07.29K4.760) along with another DNA ligase-like ORF (*LIG kβ* gene) located immediately downstream of it (Tb07.29K4.770). Both coding regions were amplified from genomic DNA (from *T. brucei* 29-13 cells) and cloned into an RNAi vector (pZJM) (34) and into expression vectors (pND1 and pND2). pND1 is a derivative of pHD496 (12) that has had the endogenous XbaI site mutated and the green fluorescent protein coding region replaced by the influenza hemagglutinin (HA) tag in triplicate. The tag sequence was inserted as a HindIII/BamHI fragment, along with an XbaI site adjacent to the HindIII site. pND2 is a derivative of pLEW100 (35) that has had the luciferase protein coding sequence replaced by the HA tag in triplicate. These constructs allow the insertion of coding regions between the HindIII and XbaI sites upstream of the 5′ end of the tag sequence (the XbaI site is in frame with the HA coding sequence).

General DNA techniques. Restriction endonuclease digests were carried out at 37°C for 1 h in the buffer recommended by the supplier (New England Biolabs, Inc., Beverly, Mass.). Fragments were separated by agarose gel electrophoresis, and DNA was extracted by using a QIAquick gel extraction kit (QIAGEN, Valencia, Calif.). Ligations were carried out with 0.5 U of T4 DNA ligase (Invitrogen, Inc., Carlsbad, Calif.) overnight at 14°C. Transformation of bacterial cells was performed by mixing 1 μl of ligation reaction mixture with 20 μl of electrocompetent TOP10 cells (Invitrogen, Inc.) and then electroporating the cells with a Cell-Porator *Escherichia coli* electroporator (Gibco BRL, Gaithersburg, Md.). Southern and Northern analyses were carried out as described previously (1). DNA sequencing was performed by cycle sequencing with fluorescent-labeled dideoxynucleoside triphosphates.

Cell growth. *T. brucei* procyclic strain YTAT 1.1 (13) was grown in SM medium (5), supplemented with 10% heat-inactivated fetal bovine serum (Gibco BRL). Strain 29-13 (35) was grown in SM medium supplemented with 15% heat-inactivated fetal bovine serum (Atlanta Biologicals, Norcross, Ga.), 32 μg of G418/ml, and 50 μg of hygromycin/ml. Cells were maintained at 28°C. Transfections were carried out as described previously (13). Briefly, cells were washed in electroporation buffer (120 mM KCl, 0.15 mM $CaCl_2$, 9.2 mM K_2HPO_4, 25 mM HEPES, 2 mM EDTA, 4.75 mM $MgCl_2$, 69 mM sucrose [pH 7.6]) and resuspended at 5×10^7 cells/ml. One hundred microliters of DNA (10 to 50 μg in water) was mixed with 450 μl of cells and electroporated by 2 pulses at 1.5 kV and 25 μF (10-s interval between pulses) in 4-mm electroporation cuvettes. Cells were allowed to recover overnight in 10 ml of medium and then put under drug selection (2.5 μg of phleomycin D1 [Zeocin; Invitrogen, Inc.]/ml) the following day. Clonal cell lines were obtained by limited dilution in 50% conditioned medium and incubated in 5% CO_2 at 28°C.

Microscopic analysis of cells during RNAi induction. Cells were removed from the tetracycline-induced culture every 24 h and fixed by addition of an equal volume of 8% paraformaldehyde. After being washed twice for 5 min in 100 mM glycine, cells were stained with 1 μg of DAPI (4′-6-diamidino-2-phenylindole; Vector Laboratories, Inc., Burlingame, Mass.)/ml in phosphate-buffered saline (PBS; 137 mM NaCl, 2.7 mM KCl, 6.5 mM Na_2HPO_4, 1.4 mM KH_2PO_4) and examined by fluorescence microscopy for DNA phenotype on a Nikon Optiphot X/Y series compound microscope. Three hundred cells were counted for each time point.

Immunofluorescence microscopy. Expression of DNA ligase kβ was constitutive in clonal stably transfected YTAT1.1 cells. Expression of DNA ligase kα was induced with 1 μg of tetracycline/ml for 6 h at 28°C in clonal, stably transfected 29-13 cells. Trypanosomes were harvested by centrifugation for 2 min at 2,000 × *g*, washed once with PBS, and resuspended at 5×10^6 cells per ml. Aliquots (100 μl) were allowed to settle onto poly-L-lysine-adherent coverslips at 4°C for 15 min. Adhered cells were fixed for 3.5 min in 4% paraformaldehyde in PBS, washed twice in 0.1 M glycine in PBS, permeabilized for 10 min in 0.025% Triton X-100 in PBS, washed twice in PBS, and then fixed overnight in −20°C methanol. Coverslips were rehydrated in PBS and blocked with 20% goat serum in PBS containing 0.05% Tween 20 for 1 h at 37°C. Primary antibodies, rabbit anti-topoisomerase II (anti-topo II) from *C. fasciculata* (1:100) (21) and mouse 12CA5 antihemagglutinin (anti-HA) (1:250) (BabCo), were allowed to bind to the coverslips in this blocking solution for 1 h at 37°C followed by washing four times in PBS containing 0.05% Tween 20. Coverslips were then incubated with secondary antibodies, Alexa Fluor 488-conjugated goat anti-mouse immunoglobulin G (1:750; Molecular Probes, Eugene, Oreg.) and Alexa Fluor 568-conjugated goat anti-rabbit immunoglobulin G (1:1,000; Molecular Probes), and washed as described above. Coverslips were then stained for 3 min in 3 μg of DAPI/ml, washed twice in PBS, and mounted in ProLong mounting medium (Molecular Probes). Images were taken with a 100×/1.4 Planapo lens on a TCS-SP MP confocal and multiphoton inverted microscope (Leica, Heidelberg, Germany) equipped with argon (488-nm blue excitation) and 561-nm (green) diode lasers and a two-photon laser setup consisting of a Spectra-Physics Millenia X 532-nm green diode pump laser and a Tsunami Ti-Sapphire picosecond-pulsed infrared laser tuned at 768 nm for UV excitation.

Analysis of cell growth and mRNA levels during RNAi induction. To monitor cell growth after RNAi induction, cultures were initiated at 2×10^5 cells/ml. Cultures were divided, and tetracycline was added to one culture at 1 μg/ml. Cells were counted daily by using a Z1 particle counter (Beckman-Coulter, Miami, Fla.). When cultures reached late log phase, they were diluted to 2×10^5 cells/ml. Growth curves are presented which account for these dilutions. Clones were also examined for the ability to knockdown target mRNA when induced with tetracycline. Cultures at 10^6 cells/ml were divided in two, and tetracycline was added to one culture to a final concentration of 1 μg/ml. Cells were harvested after 48 h, and RNA was extracted with an RNeasy miniprep kit (QIAGEN). RNA was analyzed by standard Northern blotting methods.

Fluorescence-activated cell sorter (FACS) analysis of DNA content during RNAi induction. Cells were induced with 1 μg of tetracycline/ml on consecutive days, and after 5 days, 5×10^6 cells from each culture were harvested and resuspended in 1 ml of PBS. Two microliters of 10-mg/ml dihydroethidium was added to each sample, and the samples were incubated for 5 min. Cells were harvested in a microcentrifuge, washed with PBS, and immediately analyzed in a BD-LSR analytical flow cytometer (Becton Dickenson, Franklin Lakes, N.J.) with an argon laser (488-nm excitation) and 610 (±10)-nm dichromic filter. 29-13 cells were analyzed either stained or unstained as positive and negative controls.

Total DNA isolation. Cells (3×10^7) were harvested and washed once with PBS. The cells were then resuspended in 100 mM NaCl–100 mM EDTA–10 mM Tris (pH 8.0) and lysed with 1% sodium dodecyl sulfate. The samples were digested with proteinase K and RNase A and extracted with 1:1 phenol-chloroform and with phenol-chloroform-isoamyl alcohol (25:24:1). The DNAs were ethanol precipitated and resuspended in 50 μl of 10 mM Tris-HCl (pH 8.0)–1 mM EDTA.

Analysis of free and network-associated minicircles during RNAi induction. Cells (at 8×10^5 cells/ml) were removed from culture before induction with 1 μg of tetracycline/ml and thereafter at 24-h intervals for 2 days (final cell density, 7×10^6 cells/ml). Three microliters (150 to 180 ng) of total DNA was incubated in reaction mixtures containing 10 mM Tris (pH 7.9), 50 mM NaCl, 5 mM $MgCl_2$, 1 mM EDTA, 15 μg of bovine serum albumin/ml, and 1 mM ATP with or without 7 U of topoisomerase II (USB) at 30°C for 3 h. Minicircles were analyzed by electrophoresis through a 1.5% agarose gel (1 μg of ethidium bromide/ml–90 mM Tris-borate–1 mM EDTA) for 18 h at 1.6 V/cm. Controls include 1 μl of total DNA (before induction) digested with HindIII and XbaI and 5 ng of purified kDNA from a late-log-phase culture, which had been decatenated with topo II. After washing the gel to remove ethidium bromide, the DNA was denatured with 0.5 N NaOH–1.5 M NaCl for 30 min and analyzed by Southern blotting (1). Minicircle bands were quantified with a PhosphorImager (Amersham Biosciences, Piscataway, N.J.).

Bacterial expression of DNA ligase. The coding region of *LIG kα* from amino acid numbers 12 to 483 was cloned into pET22b (Novagen) at the NdeI/XhoI sites. The resulting gene construct contained a six-His sequence in frame with the

TABLE 1. Comparison of kinetoplastid mitochondrial DNA ligases

Ligase	% Identity with protein sequence from:					
	T. brucei LIG kα	*L. major* LIG kα	*C. fasciculata* LIG kα	*T. brucei* LIG kβ	*L. major* LIG kβ	*C. fasciculata* LIG kβ
T. brucei LIG kα	100					
L. major LIG kα	41	100				
C. fasciculata LIG kα	37	58	100			
T. brucei LIG kβ	29	23	23	100		
L. major LIG kβ	29	23	22	54	100	
C. fasciculata LIG kβ	28	24	23	56	76	100

3′ end of the cloned fragment. The plasmid construct was transformed into *E. coli* BL21(DE3) cells, and protein expression was induced for 45 min at 37°C. The bacterial cells were harvested and resuspended in 20 mM Tris-HCl (pH 8.0) and protease inhibitor cocktail (Novagen). Lysozyme was added to 1 mg/ml and incubated at 30°C for 15 min. Triton X-100 was added to 1%, and NaCl was added to 0.5 M. After passage through an 18-gauge needle several times, the lysate was centrifuged at 15,000 × *g* for 15 min at 4°C and the supernatant was then filtered through a 0.45-μm-pore-size filter. The cleared lysate was loaded onto a His-Bind column (Novagen) and washed with 5 column volumes of 60 mM imidazole–0.5 M NaCl–20 mM Tris-HCl (pH 7.9). The protein was eluted in 1-ml aliquots with 0.3 M imidazole. The two peak fractions were pooled and passed over a G25 desalting column. Glycerol was added to the eluate (now in 20 mM Tris-HCl [pH 8.0], 50 mM NaCl, 1 mM dithiothreitol, 0.1 mM EDTA) to 50%, and the protein was stored at −20°C.

DNA ligase activity assay. Oligo(dT) (20-mer) was end labeled with [γ-^{32}P]ATP, purified on a G25 spin column, and then annealed to poly(dA). One hundred picograms of substrate was added to the reaction mix containing 70 mM Tris-HCl (pH 7.6), 10 mM $MgCl_2$, 5 mM dithiothreitol, and 1 mM ATP. Either His-column-purified LIG kα or an equal volume of the G25 column buffer was added to the reaction mix, and the mixture was incubated at room temperature for 2 h. The products were separated on a 6 M urea–8% polyacrylamide gel (19:1 acrylamide-bisacrylamide), which was then subsequently dried and exposed to X-ray film for autoradiography.

RESULTS

Identification of DNA ligase genes. A search of the *Leishmania major* GeneDB database revealed two ORFs that had been annotated as DNA ligases. The amino terminus of each ORF showed a potential mitochondrial localization signal. These sequences were used to identify homologues in both *C. fasciculata* (30) and *T. brucei*. Initially, a *T. brucei* gene was identified from the assembly of overlapping sequences from the EMBL genome database. The contiguous sequence was PCR amplified from *T. brucei* genomic DNA, cloned, and sequenced (GenBank accession no. AAQ72485). More recently, a chromosomal fragment containing this ORF was identified in the GeneDB database. Additionally, the chromosomal fragment contains another ORF immediately downstream of the putative DNA ligase that also has a DNA ligase motif. In all three species, two protein-encoding regions were found to be adjacent to each other on the chromosome (K. M. Sinha, unpublished data). We named these genes DNA *LIG k*α and *LIG k*β based on kinetoplast localization (30; this work) and chromosomal order.

A comparison of the kinetoplastid sequence identities is shown in Table 1. Relative to one another, the LIG kβ sequences show a level of sequence similarity often seen among these organisms (54 to 76% identity), whereas the LIG kα sequences are more divergent (37 to 58% identity). There is lower sequence similarity between LIG kα and LIG kβ (<30% identity). For both LIG kα and LIG kβ, the *L. major* and *C. fasciculata* sequences are more similar to each other than either is to the *T. brucei* sequence. The *T. brucei* ligase sequences have also been compared to other ligase sequences (Table 2). In higher eukaryotes, a gene that produces a nuclear DNA ligase, LIG III (18), also encodes the mitochondrial DNA ligase. Comparison of the *T. brucei* mitochondrial LIG kα and LIG kβ sequences to human LIG III shows that neither *T. brucei* LIG kα nor LIG kβ has significant identity to human LIG III. These sequences were also compared to two other human DNA ligases, LIG I and IV. Both human LIG I and IV are nuclear proteins. Again, the *T. brucei* LIG kα and LIG kβ have no significant identity with the human LIG I and IV (<10%). Comparison of human LIG I and IV with the equivalent protein sequences from other metazoans (*Xenopus laevis*, mouse) shows high conservation of sequence (>75% identity). As a control for these comparisons across a large evolutionary distance, the *T. brucei* LIG I was compared with the human LIG I and shows an identity of 35%. Therefore, while *T. brucei* LIG I has a common ancestry with human LIG I, *T. brucei* LIG kα and LIG kβ are not closely related to any of the DNA ligases described for humans. We suggest that *T. brucei* LIG kα and LIG kβ represent a new class of cellular DNA ligases, which we term DNA ligase k, referring to their localization in the kinetoplast.

TABLE 2. Comparison of *T. brucei* DNA ligases with DNA ligases from higher eukaryotes

Ligase	% Identity with protein sequence from:					
	T. brucei LIG kα	*T. brucei* LIG kβ	*T. brucei* LIG I	*Homo sapiens* LIG I	*Homo sapiens* LIG III	*Homo sapiens* LIG IV
T. brucei LIG kα	100					
T. brucei LIG kβ	30	100				
T. brucei LIG I	8	8	100			
Homo sapiens LIG I	6	6	35	100		
Homo sapiens LIG III	7	8	18	18	100	
Homo sapiens LIG IV	5	7	9	11	10	100

	I		III		IIIa		IV		V		VI
Hu3α	MFSEIKYDGER	-41-	MILDSEVL	-28-	CLFVFDCIYFND	-52-	EGLVL	-13-	WLKVKKDYLNE	-121-	PRCTRIRDDK
Mu3α	MFAEIKYDGER	-41-	MILDSEVL	-28-	CLFVFDCIYFND	-52-	EGLVL	-13-	WLKVKKDYLNE	-122-	PRCTRIRDDK
Xl3α	MYAEIKYDGER	-41-	MILDAEVL	-28-	CLFVFDCIYFNG	-52-	EGLVL	-13-	WLKVKKDYLNE	-121-	PRCTRFRDDK
Tbkα	LFVSPKLDGVR	-41-	LVLDGELY	-32-	QYHVFDLLYAKE	-60-	EGIMI	-35-	LLKYKLMQDSE	-64-	PRFPIGKCVR
Lmkα	LQVSPKLDGIR	-42-	LVLDGELY	-97-	QYHVFDVLYSRE	-66-	EGVMI	-58-	LLKYKVMQDAE	-66-	PRFPVGKCVR
Cfkα	IRVSPKLDGIR	-42-	LVLDGELY	-99-	QYHVFDVLYARE	-66-	EGAMI	-43-	LLKYKVMQDAE	-66-	PRFPIGKSVR
Tbkβ	LLVSPKIDGIR	-41-	LLLDGELF	-32-	EYFAFDIMASDQ	-80-	EGVII	-15-	LLKYKYMHDAE	-64-	PRFPIAKCVR
Lmkβ	LLASPKIDGIR	-41-	LMLDGELF	-32-	EYFAFDIMYSAQ	-85-	EGVMI	-15-	LLKYKQMHDAE	-64-	PRFPIAKAIR
Cfkβ	MLASPKIDGIR	-41-	LMLDGELF	-32-	EYFAFDIMYSAQ	-84-	EGVMI	-15-	LLKYKQMHDAE	-64-	PRFPVAKAVR

FIG. 1. Conservation of DNA ligase motifs in mitochondrial DNA ligases. Six colinear sequence elements conserved in ATP-dependent DNA ligases are compared between trypanosomatid and vertebrate mitochondrial DNA ligases. The aligned sequences are from human ligase IIIα (Hu3α), mouse ligase IIIα (Mu3α), *Xenopus* ligase IIIα (Xl3α), *T. brucei* ligase kα (Tbkα), *T. brucei* ligase kβ (Tbkβ), *L. major* ligase kα (Lmkα), *L. major* ligase kβ (Lmkβ), *C. fasciculata* ligase kα (Cfkα), and *C. fasciculata* ligase kβ (Cfkβ). Conserved amino acid residues are indicated by shading.

DNA ligase motifs. GTP-dependent capping enzymes and ATP-dependent DNA ligases make up a superfamily of covalent nucleotidyltransferases with six characteristic motifs (32). Figure 1 shows an alignment of these motifs in mitochondrial DNA ligases from vertebrates and kinetoplastid protozoa. The adenylated moiety is covalently bound to the lysine residue within a conserved KxDG element in motif I. Even around the active site lysine, the kinetoplastid ligases show limited sequence similarity to those of the mitochondrial ligases of vertebrates.

Kinetoplast localization of ligase proteins. Epitope tagging was used to confirm the mitochondrial localization of *T. brucei* LIG kα and LIG kβ. The coding region of *LIG kα* was cloned into pND2, a derivative of the pLEW100 expression vector (35) containing three copies of the HA epitope tag. Stably integrated 29-13 cell lines containing pND2:LIGkα were cloned, expression was induced, and cells were immunostained with anti-HA monoclonal antibodies and polyclonal antibodies against the *C. fasciculata* topoisomerase II (Fig. 2). The anti-HA antibodies show staining that overlaps the DAPI fluorescence of the kDNA, suggesting that the LIG kα is present throughout the kDNA disk. We note that the localization of the two points of fluorescence due to that of topo II here is not at the opposite edges of the kDNA disk as seen for *C. fasciculata* (21) but appears closer to the flagellar face of the disk and with a separation slightly less than the width of the disk. The ORF for *LIG kβ* was introduced into pND1, a derivative of the pHD496 expression vector (3) containing three copies of the HA epitope tag, used to stably transfect YTAT1.1 cells with the linearized construct (pND1:LIGkβ), and then cloned. Immunofluorescence localization of LIG kβ in these cells with anti-HA monoclonal antibodies shows antipodal localization of LIG kβ at the edges of the kDNA disk but overlapping the localization of topo II only slightly (Fig. 3). This localization of LIG kβ differs from that of the *C. fasciculata* DNA LIG kβ, where the ligase was found to localize to the antipodal sites and, to a lesser extent, to the faces of the kDNA disk (30).

RNA interference. In light of the kinetoplast localization of these ligase proteins, their function was analyzed by eliminating gene expression with RNAi. Each gene was found to be single copy by Southern blot analysis (data not shown), and the entire coding region of each gene was cloned into the tetracycline-inducible RNAi vector pZJM (34). The resulting plasmids pZJM:LIGkα and pZJM:LIGkβ were linearized and electroporated into procyclic 29-13 cells. After selection, limiting dilution produced clonal cell lines. Several clones were examined for their ability to induce RNAi. Figure 4A shows the growth curve and Northern blot analysis of a typical clone for pZJM:LIGkβ. Clearly, there is no effect on either the growth or even levels of the *LIG kβ* mRNA upon induction with tetracycline (Fig. 4A, inset). This insensitivity to RNAi

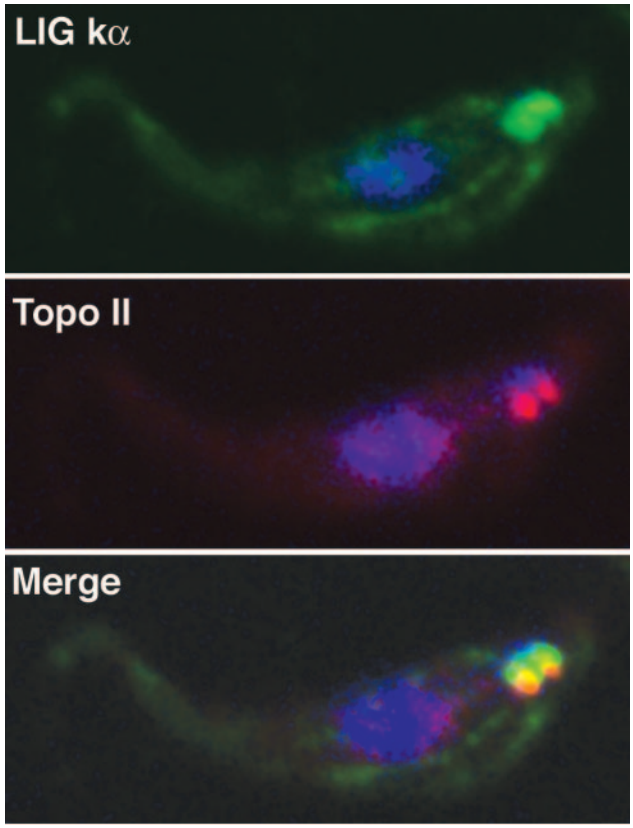

FIG. 2. Localization of epitope-tagged DNA LIG kα. Cloned cells expressing HA-tagged DNA LIG kα were fixed and permeabilized on coverslips and then incubated with anti-HA monoclonal antibodies (12CA5) and rabbit polyclonal antibodies against the *C. fasciculata* kinetoplast topo II. The cells were then incubated with secondary antibodies (goat anti-mouse Alexa 488 and goat anti-rabbit 568). The coverslips were washed, incubated with DAPI, and then mounted with mounting medium. The images were captured on a Leica TCS-SP MP confocal and multiphoton inverted microscope. The LIG kα (green) and topo II (red) localizations are shown relative to those of the nuclear and kinetoplast DNAs (blue).

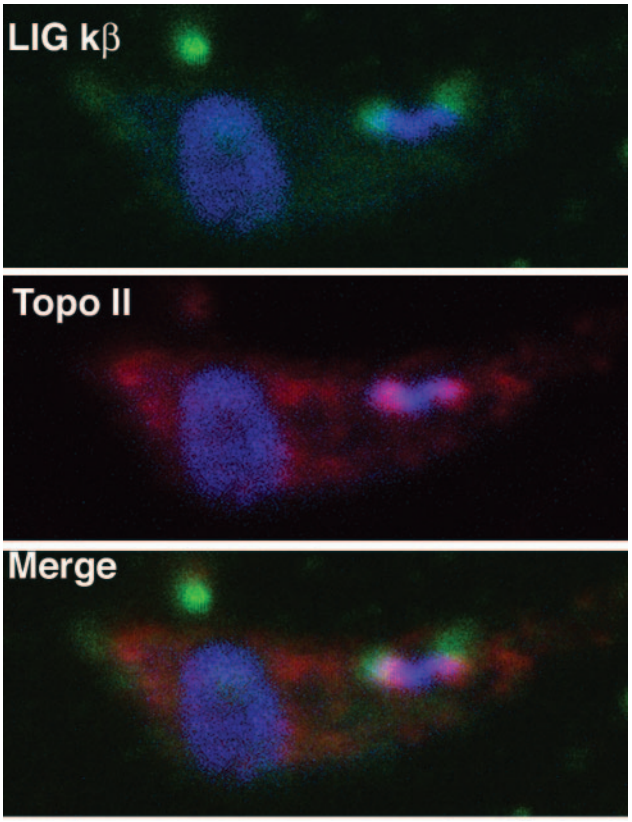

FIG. 3. Localization of epitope-tagged LIG kβ. Cloned cells expressing LIG kβ were immunostained and examined by confocal microscopy as described in the legend to Fig. 2.

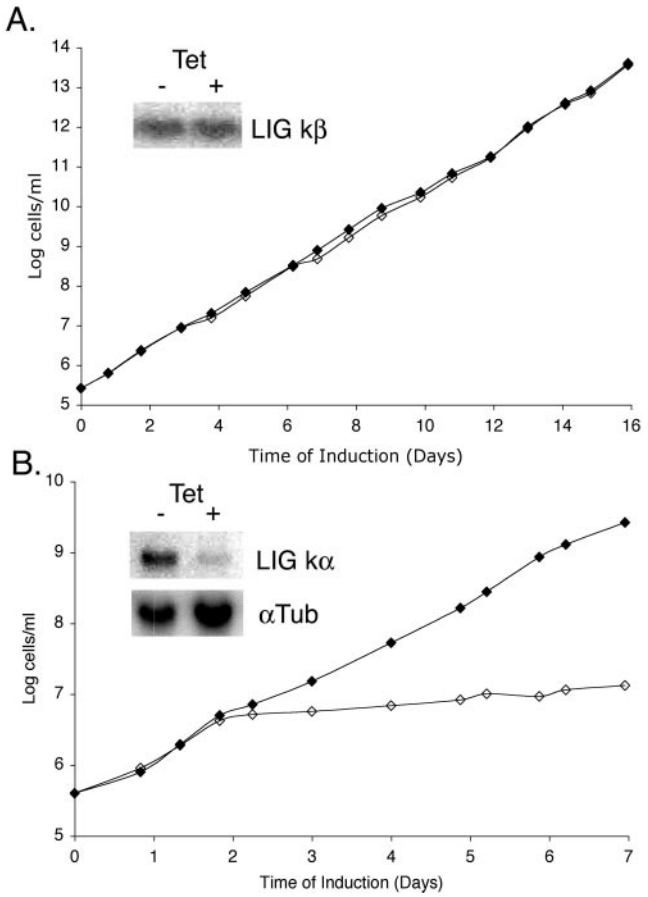

FIG. 4. RNAi of *T. brucei* mitochondrial DNA ligases. (A) RNAi of *LIG k*β; (B) RNAi of *LIG k*α. Cells were grown in the absence (filled diamond) or presence (open diamond) of tetracycline (1 μg/ml). The concentration of cells was determined each day, and cultures were diluted to maintain log phase. (Inset) Northern analysis of RNAi induction. Cells were grown in the absence (−) or presence (+) of tetracycline (Tet) for 48 h. The blot was also probed for α-tubulin genes as a loading control.

was found for 10 independent clones. The basis for this insensitivity has not yet been investigated.

Similar experiments were performed with clones of the pZJM:LIGkα transfection. Figure 4B (upper inset) shows a Northern blot analysis of clonal cells that had been either mock treated or treated with tetracycline for 48 h. The blot was reprobed with α-tubulin coding sequence to compare loading of the lanes (lower inset). Despite approximately twofold overloading of the RNA from induced cells, a clear decrease (>90%) in *LIG k*α mRNA can be seen compared to that of the uninduced cells. Figure 4B also shows the growth curve of clonal pZJM:LIGkα cells in the absence or presence of tetracycline. While cells grow normally in the absence of tetracycline, within 3 days of treatment with tetracycline, cell growth is arrested, indicating that *LIG k*α is an essential gene. The onset of inhibition of cell division was detectable within six doublings. This rapid onset of growth phenotype also suggests that the protein may be rapidly turned over.

Loss of kDNA by silencing of LIG kα. Cells were also examined by fluorescence microscopy during RNAi induction. Cells were removed from the culture every 24 h and stained with DAPI to allow visualization of both the nucleus and kinetoplast. Cells demonstrated a variety of typical phenotypes that can be designated as one of 4 groups, normal (containing 1k/1n, 2k/1n or 2k/2n), anucleate (containing 1k/0n), no kDNA (1n, 2n), or monster (more than 2k and/or 2n). Within the normal group was a subset in which the kDNA appeared much smaller than usual. These cells were only seen with a single kinetoplast (for example, the second normal cell in Fig. 5A). The percentage of each phenotype is shown in Fig. 5B. The relative proportion of each phenotype was the same in wild type 29-13 cells as in the uninduced clonal cells (data not shown). However, within 24 h of induction, the number of cells with no detectable kDNA had started to increase and by 48 h equaled the number of normal cells. Beyond this point, the number of cells lacking any detectable kinetoplast reached as much as 85% of the population. The rapid loss of kDNA mirrors the cessation of growth in the culture. One caveat is that some of these cell phenotypes (especially the anucleate cells) may not survive long. Therefore, it is possible that the frequencies of these phenotypes are underestimated in the population because they die before they can be accurately quantified. If the RNAi induction is continued, the cells lacking kDNA appear to decrease in number. Between days 5 and 8, we see a recovery in the number of cells with a kDNA disk. This recovery may be a consequence of cells with no kDNA dying within 48 h. Therefore, only cells with newly lost kDNA

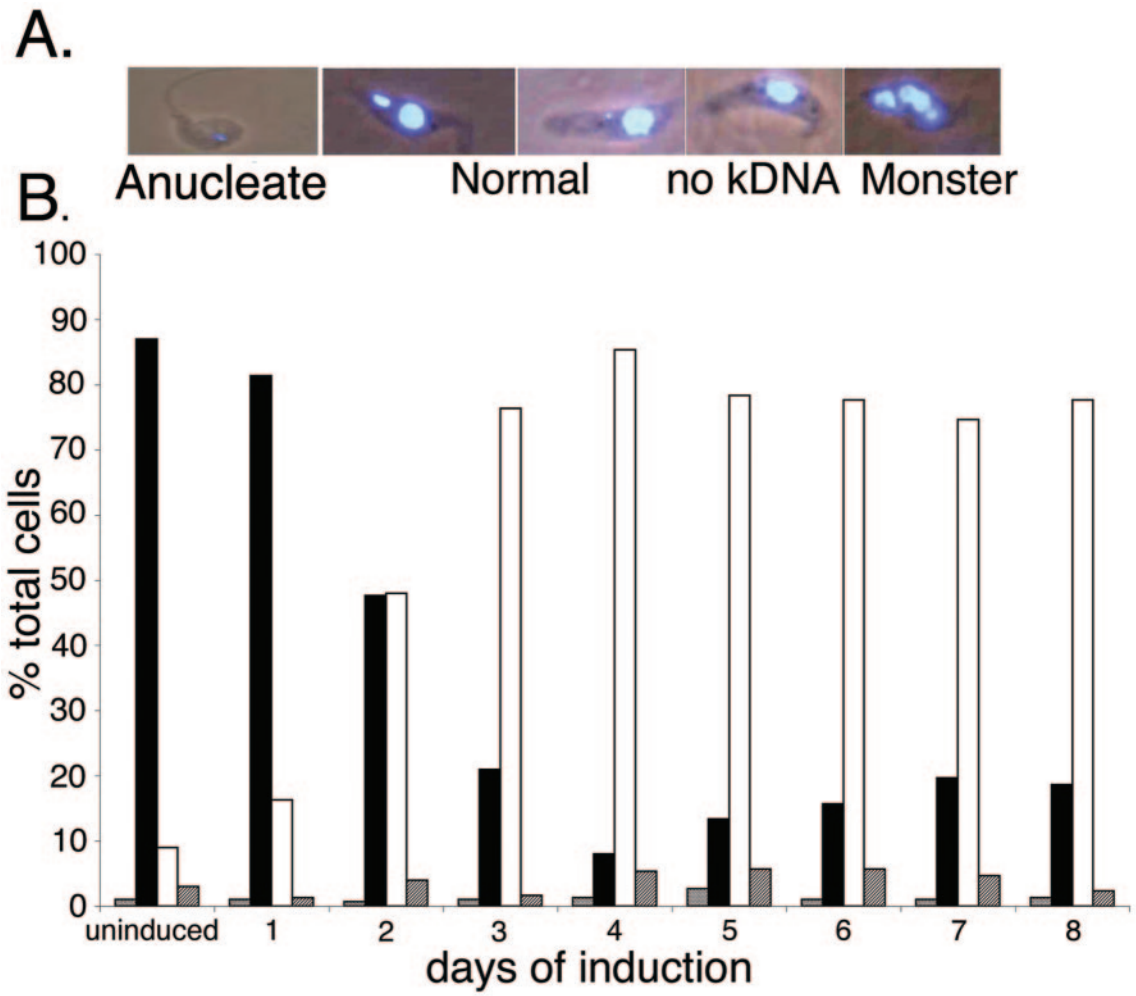

FIG. 5. Cell phenotype during *LIG kα* RNAi induction. Cells were induced with tetracycline, and on subsequent days, samples were removed, fixed, and stained with DAPI. Cells were scored by kDNA and nuclear phenotype. (A) Examples of phenotypes scored are as follows: anucleate, cells with no nucleus but with a kinetoplast; normal, cells with a nucleus and kinetoplast; no kDNA, cells with a nucleus but no kinetoplast; monster, cells with multiple nuclei and/or kinetoplasts. (B) Graph representing the observed frequency of each phenotype. The number of cells with a particular phenotype is expressed as a percentage of the total cells for that time point. Grey, anucleate; black, normal; white, no kDNA; diagonal stripes, monster.

disks or with some form of kDNA disk survive beyond the first few days of induction.

Accumulation of form II minicircles in kDNA networks. In light of the loss of the kDNA upon induction of *LIG kα* RNAi, the populations of free and network-associated minicircles were examined in clonal cells treated with tetracycline. At 0, 24, and 48 h after the addition of tetracycline, cells were removed from the culture and total DNA (with and without treatment with topoisomerase II) from equivalent numbers of cells was analyzed by Southern blotting (Fig. 6). kDNA networks do not enter the gel, and consequently, in the untreated samples only free minicircles migrate through the gel and are detected by Southern blotting. In samples treated with topoisomerase II, the network-associated minicircles are also released and detected on the blot. A chromosomal DNA signal near the top of the gel was used as a loading control to ensure that similar cell equivalents were present in each lane. Prior to RNAi induction (day 0), the free minicircles are observed as covalently closed circles (form I) and nicked circles (form II). Linear molecules (form III) are also seen in the control DNA in lane 1. In the topoisomerase-treated samples from uninduced cells (lane 4), the network-associated minicircles are present in the lane in addition to the free minicircles. The higher bands in lane 4 represent catenanes. After 1 day of induction of RNAi, free form I minicircles are no longer present and the amount of free form II minicircles is greatly reduced. The relative amounts of network-associated form I and form II minicircles can be estimated by subtracting the amounts of each form in the untreated lanes from the amounts of the corresponding form in the treated lanes (assuming that the relative amounts of form I and form II in the catenanes is the same as that of the released minicircles). Form I minicircles accounted for 66% of the network-associated minicircles prior to induction of RNAi. By 1 day of induction, there were no longer any free form I minicircles and form I minicircles represented only 28% of the network-associated

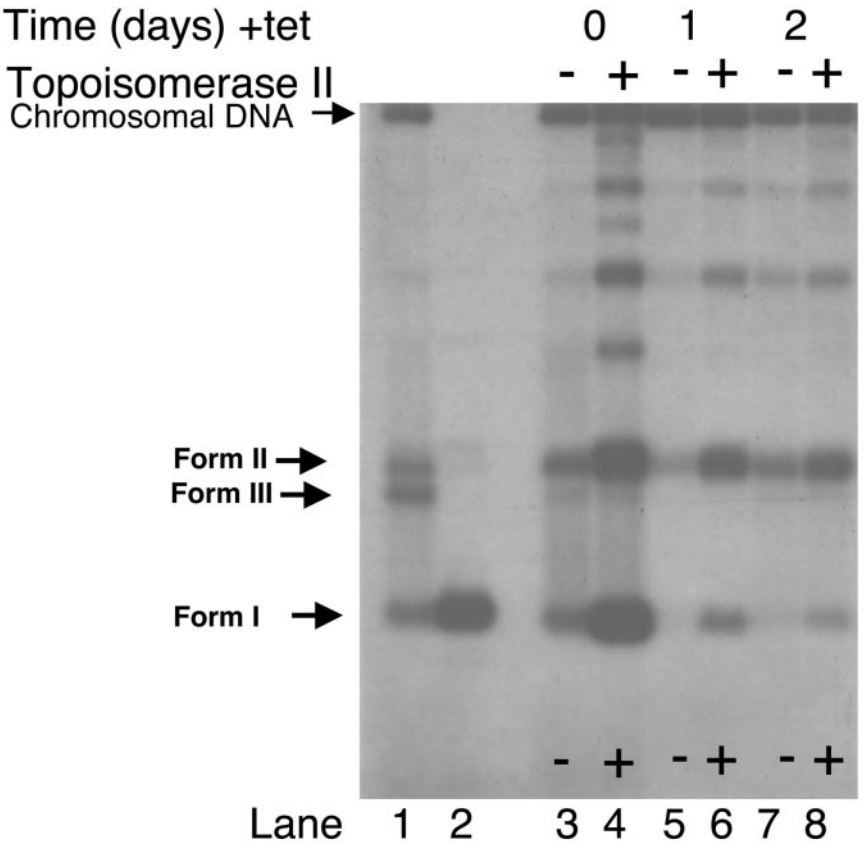

FIG. 6. Southern analysis of free and network-associated minicircles during *LIG kα* RNAi induction. Total cellular DNA was isolated from cells at 0, 1, and 2 days after the addition of tetracycline (tet). Equal cell equivalents of the DNA with (+) or without (−) treatment with topoisomerase II were analyzed on a 1.5% agarose gel. After blotting the gel, the membrane was probed with a minicircle probe. Form I, covalently closed minicircles; form II, relaxed minicircles; form III, linear minicircles. Markers: lane 1, day 0 DNA treated with HindIII and XbaI; lane 2, purified kDNA treated with topoisomerase II.

minicircles. By day 2, form I minicircles represented only approximately 18% of the network-associated minicircles. We interpret these results to indicate that free minicircles continue to be reattached to the network in the absence of L1G kα function and that, as nascent network-associated minicircles fail to be covalently closed, the amount of form I minicircles is quickly diminished and the networks accumulate form II minicircles.

Shrinkage of kDNA. The loss of kDNA was examined further by FACS analysis of cells stained with dihydroethidium. Dihydroethidium is taken up by the mitochondria and oxidized to ethidium and, consequently, specifically stains the kDNA (33). FACS analysis of cells treated with tetracycline for different amounts of time and stained with dihydroethidium is shown in Fig. 7. Relative fluorescence intensity is on the *x* axis and is directly proportional to the amount of kDNA. The *y* axis measures the number of cells counted at a particular fluorescence intensity. The stained cells show a broad peak representing a range of kDNA sizes in the exponential culture. The staining intensity pattern for uninduced cells approximates the staining intensity pattern for stained 29-13 cells (data not shown). By day 3 of tetracycline treatment, the peak of fluorescence has moved to approximately half the value of the day 0 cells, indicating a reduced content of kDNA in the cells. By day 5, the major peak is almost as low as that of unstained 29-13 cells (data not shown), indicating that most of the treated cells have little or no kDNA. These observations are consistent with our microscopic examination of DAPI-stained cells showing shrinkage and loss of kDNA during RNAi induction.

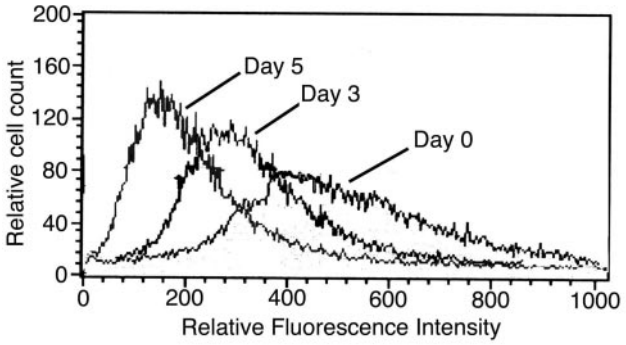

FIG. 7. FACS analysis of *LIG kα* RNAi induced cells. Cells from 0, 3, and 5 days of induction were stained with dihydroethidium and analyzed on a BD LSR analytical flow cytometer. The resulting plot shows the relative fluorescence intensity versus the relative cell count.

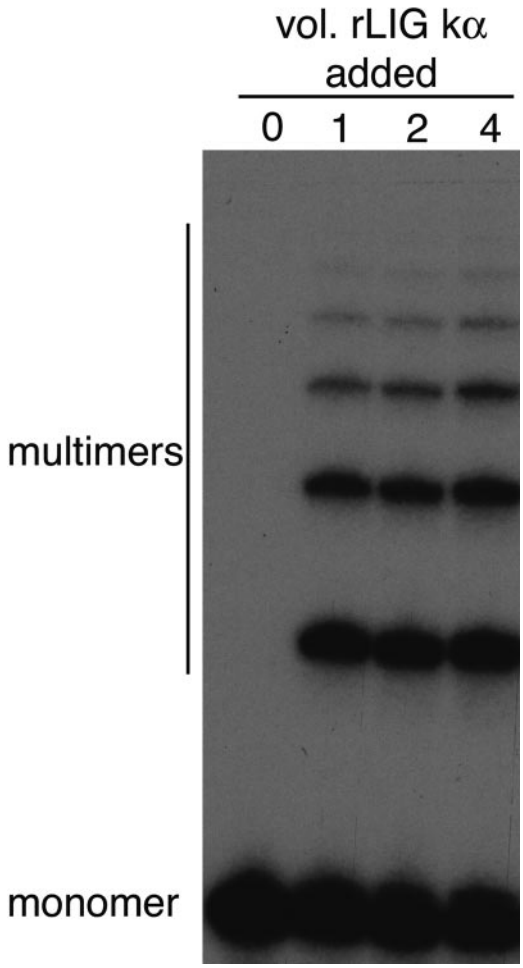

FIG. 8. DNA ligase activity of LIG kα. Autoradiograph of reaction products electrophoresed on a denaturing acrylamide gel. 5′ end-labeled oligo(dT) was annealed to a poly(dA) backbone and incubated either alone (0) or with increasing amounts (1, 2, and 4 μl) of the purified recombinant LIG (rLIG) kα. Ligation reactions contained 1 mM ATP. vol., volume.

Enzymatic activity of LIG kα. Because the *LIG k*α RNAi induction showed such a strong effect on mitochondrial DNA maintenance, it was important to confirm the ligase activity of LIG kα. The LIG kα was expressed in *E. coli* as a His-tagged recombinant protein to allow purification of the trypanosomal protein for biochemical analysis. Although the tagged protein was strongly induced, almost all of the protein was contained in inclusion bodies. There was, however, enough protein soluble to purify by metal chelate chromatography and to assay for activity following desalting by chromatography on Sephadex G25. A radiolabeled synthetic substrate consisting of a poly(dA) strand hybridized to ^{32}P-labeled oligo(dT) was used to assay ligation of the adjacent oligo(dT) molecules into higher-molecular-weight products by using ATP as cofactor. Possible contamination of the recombinant protein by *E. coli* ligase is excluded based on the purification by metal chelate chromatography and the requirement for NAD as a cofactor by *E. coli* DNA ligase. Figure 8 shows the result of adding increasing amounts of the recombinant protein to the ligase reaction mixture. The reaction mix was separated on a denaturing polyacrylamide gel, allowing the identification of ligated multimers of the oligo(dT).

DISCUSSION

The present model (22) for trypanosomal mitochondrial DNA (kDNA) replication implies the existence of two kinetoplast DNA ligase activities, separated by both location and time of functioning. The first activity would be antipodal on the kDNA disk, colocalizing with other replication and repair enzymes and involved in the joining of Okazaki fragments on nascent minicircles. The second would be localized throughout the network and involved in the closure of discontinuities at minicircle replication origins prior to the cleavage of the double-size kDNA network. While it would be possible for these activities to be carried out by the same protein, in this report we have described two new and unique DNA ligases localized to the kDNA disk of *T. brucei*. The localization of each protein is consistent with separate roles in kDNA replication.

The genome databases for several trypanosomatid species are fast nearing completion, and the initial annotation is a rich new source of data to be analyzed. Despite a lack of overall sequence similarity between these new DNA ligase sequences (*LIG k*α and *LIG k*β) and other ligase genes, there is enough homology in the conserved ligase motifs to allow identification. The evolutionary distance between these and other DNA ligases allows for large sequence drift in regions of the proteins not constrained by specific functional needs, e.g., the active site lysine and adjacent residues required for adenylation. It should be noted that additional kDNA-associated DNA ligases could be present in trypanosomatids. Although the two proteins we describe are sufficient for the present model of kDNA replication, we have only to look at the case of DNA polymerases to see a precedent for numerous genes. There are at least 4 DNA polymerase I-like proteins localized to the mitochondrion (17) plus 2 DNA polymerase β-like proteins (27).

As with all database identification, it is essential to confirm the activity of the protein by biochemical assay. This activity of LIG kβ has been demonstrated recently for the *C. fasciculata* protein (30). The ligase activity of the *T. brucei* LIG kα has been demonstrated here based on its ability to ligate oligo(dT) molecules annealed to a poly(dA) backbone.

Both the LIG kα and LIG kβ proteins are transported to the mitochondrion of *T. brucei*. The LIG kβ showed discreet localization at the antipodal sites of the kDNA similar to that observed with the LIG kβ of *C. fasciculata* but does not also show additional localization to the faces of the kDNA as seen in *C. fasciculata* (30). Since the localization of LIG kβ in *C. fasciculata* involved episomal expression of the epitope-tagged protein, we cannot exclude the possibility that localization to the faces of the kDNA disk resulted as a consequence of possible overexpression of LIG kβ. It is of particular interest to note here that the *T. brucei* LIG kβ and topo II do not colocalize. These proteins appear to be in adjacent structures or complexes at the opposite edges of the kDNA disk. The spatial separation of these proteins could have a functional purpose. Perhaps nascent minicircles must be processed through a complex of replication proteins and then reattached to the kDNA network by an adjacent complex containing the topoisomerase.

Such a conveyer belt type of mechanism could assure that nascent minicircles are only reattached to the network following their replication.

The use of inducible RNAi is now common practice in the analysis of gene function in *T. brucei* (31). This approach allows the analysis of potentially essential genes by knocking down expression of the mRNA in the cell. Several different strategies exist for the expression of the double-stranded RNA. We have chosen to utilize the opposing promoter plasmid pZJM created by Wang et al. (34). This construct allows the insertion of the gene of interest between two opposing T7 promoters that are controlled by tetracycline repressors. Here we have described attempts to knockdown expression of the *LIG k*α and *LIG k*β genes. Unfortunately, despite screening 10 clones transfected with the pZJM:LIGkβ vector, no reduction of *LIG k*β mRNA was observed upon addition of tetracycline. The reason for the lack of an effect of RNAi in this case is unclear and remains to be investigated.

On the other hand, RNAi effectively knocked down the mRNA for the *LIG k*α. Northern blot analysis showed a reduction in mRNA of at least 90% within 48 h of induction with tetracycline. The effect appears to be extremely rapid, as the molecular phenotype of LIG kα depletion was apparent within 24 h. Although the growth curve suggests that cells will continue to grow at a normal rate for 3 days, there are significant changes in both the free minicircle population and the kDNA content of the cells sooner.

LIG kα appears to be present throughout the kDNA. Since the nicked and gapped daughter minicircles in a network preparing for division exist throughout the network, the localization of LIG kα is consistent with a role in the final sealing of the form II minicircles prior to division of the network. The accumulation of form II minicircles in the kDNA networks in cells in which LIG kα expression has been knocked down is also consistent with this possibility. The rapid loss of form I minicircles from both the free minicircle pool and from the kDNA networks suggests that as form I minicircles are released from the network and replicated they become reattached to the networks as form II minicircles, leading to the accumulation of form II minicircles in the networks and depletion of form I in both the pool of free minicircles and network-associated minicircles.

The average size of the kinetoplasts, based on FACS analysis, is also reduced following induction of RNAi against LIG kα. This result suggests that cells having an incompletely repaired kDNA network can nonetheless continue to divide, at least in the short term. The observation that RNAi-induced cells continue to divide and, in the process, segregate the incompletely repaired kDNA suggests that the inhibition of ligation of discontinuities in the reattached minicircles isn't required for division of the kDNA network. Division of the kDNA networks in the absence of continued kDNA replication would halve the amount of kDNA in each daughter cell. Microscopic examination of the kinetoplasts by DAPI staining of the cells after RNAi induction shows that the kinetoplasts quickly become reduced in size and are lost from the cells. The rapid appearance of cells with no detectable kDNA may result from an asymmetric division in which one cell retains the kinetoplast and the other daughter cell lacks a kinetoplast. A minimum size of the kinetoplast may be necessary for its division, and below that size, perhaps only one of the daughter cells retains the kinetoplast at cell division. This interpretation is consistent with earlier observations with *T. brucei* cells in which topoisomerase II expression was silenced (33). Network shrinkage occurred and was followed by asymmetrical division of the networks, leading to one of the daughter cells having insufficient kDNA to provide the complete repertoire of minicircles encoding guide RNAs essential for RNA editing.

In addition to confirming the presence of two DNA ligases associated with the kinetoplast, the description of the LIG kα protein may open new avenues for addressing the mechanisms of control for the terminal steps in replication of the kDNA network. Protein interaction studies should allow identification of proteins involved in this process.

ACKNOWLEDGMENTS

We thank Kent Hill for providing both the pHD496 plasmid and *T. brucei* YTAT 1.1 procyclic cells and for use of the Zeiss Axiom microscope, Paul Englund for providing the pZJM vector, George A. Cross for providing *T. brucei* 29-13 procyclic cells, and Matthew Schibier for performing the confocal microscopy in the Carol Moss Spivak Imaging Facility in the UCLA Brain Research Institute.

Flow cytometry was performed in the UCLA Jonsson Comprehensive Cancer Center and Center for AIDS Research Flow Cytometer Core Facility supported by National Institutes of Health awards CA-16042 and AI-28687, by the Jonsson Center, the UCLA AIDS Institute, and the UCLA School of Medicine. This research was supported by NIH grant GM53254.

REFERENCES

1. **Avliyakulov, N. K., J. Lukes, and D. S. Ray.** 2004. Mitochondrial histone-like DNA-binding proteins are essential for normal cell growth and mitochondrial function in *Crithidia fasciculata*. Eukaryot. Cell **3:**518–526.
2. **Barrett, M. P., R. J. Burchmore, A. Stich, J. O. Lazzari, A. C. Frasch, J. J. Cazzulo, and S. Krishna.** 2003. The trypanosomiases. Lancet **362:**1469–1480.
3. **Biebinger, S., S. Rettenmaier, J. Flaspohler, C. Hartmann, J. Pena-Diaz, L. E. Wirtz, H. R. Hotz, J. D. Barry, and C. Clayton.** 1996. The PARP promoter of *Trypanosoma brucei* is developmentally regulated in a chromosomal context. Nucleic Acids Res. **24:**1202–1211.
4. **Birkenmeyer, L., H. Sugisaki, and D. S. Ray.** 1987. Structural characterization of site-specific discontinuities associated with replication origins of minicircle DNA from *Crithidia fasciculata*. J. Biol. Chem. **262:**2384–2392.
5. **Cunningham, I.** 1977. New culture medium for maintenance of tsetse tissues and growth of trypanosomatids. J. Protozool. **24:**325–329.
6. **Drew, M. E., and P. T. Englund.** 2001. Intramitochondrial location and dynamics of *Crithidia fasciculata* kinetoplast minicircle replication intermediates. J. Cell Biol. **153:**735–744.
7. **Engel, M. L., and D. S. Ray.** 1999. The kinetoplast structure-specific endonuclease I is related to the 5′ exo/endonuclease domain of bacterial DNA polymerase I and colocalizes with the kinetoplast topoisomerase II and DNA polymerase beta during replication. Proc. Natl. Acad. Sci. USA **96:**8455–8460.
8. **Englund, P. T.** 1979. Free minicircles of kinetoplast DNA networks in *Crithidia fasciculata*. J. Biol. Chem. **254:**4895–4900.
9. **Ferguson, M., A. F. Torri, D. C. Ward, and P. T. Englund.** 1992. In situ hybridization to the *Crithidia fasciculata* kinetoplast reveals two antipodal sites involved in kinetoplast DNA replication. Cell **70:**621–629.
10. **Guilbride, D., and P. Englund.** 1998. The replication mechanism of kinetoplast DNA networks in several trypanosomatid species. J. Cell Sci. **111:**675–679.
11. **Gull, K.** 2001. The biology of kinetoplastid parasites: insights and challenges from genomics and post-genomics. Int. J. Parasitol. **31:**443–452.
12. **Hill, K. L., N. R. Hutchings, P. M. Grandgenett, and J. E. Donelson.** 2000. T lymphocyte-triggering factor of African trypanosomes is associated with the flagellar fraction of the cytoskeleton and represents a new family of proteins that are present in several divergent eukaryotes. J. Biol. Chem. **275:**39369–39378.
13. **Hill, K. L., N. R. Hutchings, D. G. Russell, and J. E. Donelson.** 1999. A novel protein targeting domain directs proteins to the anterior cytoplasmic face of the flagellar pocket in African trypanosomes. J. Cell Sci. **112:**3091–3101.
14. **Hines, J. C., M. L. Engel, H. Zhao, and D. S. Ray.** 2001. RNA primer removal and gap filling on a model minicircle replication intermediate. Mol. Biochem. Parasitol. **115:**63–67.
15. **Holder, A. A., and G. A. Cross.** 1981. Glycopeptides from variant surface

glycoproteins of *Trypanosoma brucei*. C-terminal location of antigenically cross-reacting carbohydrate moieties. Mol. Biochem. Parasitol. **2:**135–150.
16. **Klingbeil, M. M., M. E. Drew, Y. Liu, J. C. Morris, S. A. Motyka, T. T. Saxowsky, Z. Wang, and P. T. Englund.** 2001. Unlocking the secrets of trypanosome kinetoplast DNA network replication. Protist **152:**255–262.
17. **Klingbeil, M. M., S. A. Motyka, and P. T. Englund.** 2002. Multiple mitochondrial DNA polymerases in *Trypanosoma brucei*. Mol. Cell **10:**175–186.
18. **Lakshmipathy, U., and C. Campbell.** 1999. The human DNA ligase III gene encodes nuclear and mitochondrial proteins. Mol. Cell. Biol. **19:**3869–3876.
19. **Lukes, J., D. L. Guilbride, J. Votypka, A. Zikova, R. Benne, and P. T. Englund.** 2002. Kinetoplast DNA network: evolution of an improbable structure. Eukaryot. Cell **1:**495–502.
20. **Madison-Antenucci, S., J. Grams, and S. L. Hajduk.** 2002. Editing machines: the complexities of trypanosome RNA editing. Cell **108:**435–438.
21. **Melendy, T., C. Sheline, and D. S. Ray.** 1988. Localization of a type II DNA topoisomerase to two sites at the periphery of the kinetoplast DNA of *Crithidia fasciculata*. Cell **55:**1083–1088.
22. **Morris, J. C., M. E. Drew, M. M. Klingbeil, S. A. Motyka, T. T. Saxowsky, Z. Wang, and P. T. Englund.** 2001. Replication of kinetoplast DNA: an update for the new millennium. Int. J. Parasitol. **31:**453–458.
23. **Ntambi, J. M., and P. T. Englund.** 1985. A gap at a unique location in newly replicated kinetoplast DNA minicircles from *Trypanosoma equiperdum*. J. Biol. Chem. **260:**5574–5579.
24. **Perez-Morga, D., and P. T. Englund.** 1993. The structure of replicating kinetoplast DNA networks. J. Cell Biol. **123:**1069–1079.
25. **Perez-Morga, D. L., and P. T. Englund.** 1993. The attachment of minicircles to kinetoplast DNA networks during replication. Cell **74:**703–711.
26. **Robinson, D. R., and K. Gull.** 1994. The configuration of DNA replication sites within the *Trypanosoma brucei* kinetoplast. J. Cell Biol. **126:**641–648.
27. **Saxowsky, T. T., G. Choudhary, M. M. Klingbeil, and P. T. Englund.** 2003. *Trypanosoma brucei* has two distinct mitochondrial DNA polymerase beta enzymes. J. Biol. Chem. **278:**49095–49101.
28. **Simpson, L., R. Aphasizhev, G. Gao, and X. Kang.** 2004. Mitochondrial proteins and complexes in Leishmania and Trypanosoma involved in U-insertion/deletion RNA editing. RNA **10:**159–170.
29. **Simpson, L., S. Sbicego, and R. Aphasizhev.** 2003. Uridine insertion/deletion RNA editing in trypanosome mitochondria: a complex business. RNA **9:**265–276.
30. **Sinha, K. M., J. C. Hines, N. Downey, and D. S. Ray.** 2004. Mitochondrial DNA ligase in *Crithidia fasciculata*. Proc. Natl. Acad. Sci. USA **101:**4361–4366.
31. **Ullu, E., C. Tschudi, and T. Chakraborty.** 2004. RNA interference in protozoan parasites. Cell. Microbiol. **6:**509–519.
32. **Wang, S. P., L. Deng, C. K. Ho, and S. Shuman.** 1997. Phylogeny of mRNA capping enzymes. Proc. Natl. Acad. Sci. USA **94:**9573–9578.
33. **Wang, Z., M. E. Drew, J. C. Morris, and P. T. Englund.** 2002. Asymmetrical division of the kinetoplast DNA network of the trypanosome. EMBO J. **21:**4998–5005.
34. **Wang, Z., J. C. Morris, M. E. Drew, and P. T. Englund.** 2000. Inhibition of *Trypanosoma brucei* gene expression by RNA interference using an integratable vector with opposing T7 promoters. J. Biol. Chem. **275:**40174–40179.
35. **Wirtz, E., S. Leal, C. Ochatt, and G. A. Cross.** 1999. A tightly regulated inducible expression system for conditional gene knock-outs and dominant-negative genetics in *Trypanosoma brucei*. Mol. Biochem. Parasitol. **99:**89–101.